

## 2p x-ray absorption of 3d transition-metal compounds: An atomic multiplet description including the crystal field

F. M. F. de Groot and J. C. Fuggle

*Research Institute for Materials, University of Nijmegen, Toernooiveld, 6525 ED Nijmegen, The Netherlands*

B. T. Thole and G. A. Sawatzky

*Materials Science Centre, University of Groningen, Nijenborgh 18, Paddepoel, 9747 AG Groningen, The Netherlands*

(Received 30 January 1990; revised manuscript received 4 June 1990)

The metal 2p x-ray-absorption spectra (or  $L_{2,3}$  edges) of 3d transition-metal compounds are calculated, using atomic multiplet theory with inclusion of the cubic crystal field. A general overview of the effect of the cubic crystal field on the shape of the  $3d^N$  to  $2p^5 3d^{N+1}$  excitation spectrum is given for 14 common valencies of 3d transition-metal ions. Comparison to some high-resolution 2p x-ray-absorption spectra shows excellent agreement, which confirms the validity of the approach. Possible refinements of the theory, including lower-symmetry calculations and the inclusion of configuration interaction, are discussed.

### I. INTRODUCTION

As a result of the experimental progress in the field of (soft-) x-ray-absorption spectroscopy (XAS), the attainable resolution has improved to its present best value of 1:10 000.<sup>1</sup> The high-resolution 2p x-ray-absorption spectra of transition-metal compounds show a large amount of structure at the edge, which now can be investigated in detail. In this paper we present a theoretical analysis of these spectra, based on atomic multiplet theory with the inclusion of the cubic crystal field. A similar method has been used by Yamaguchi *et al.*<sup>2</sup>

We summarize briefly the general description of the absorption process to clarify the difference of our approach with the more common single-particle density of states (DOS) and multiple-scattering approaches. The x-ray-absorption cross section is given by<sup>3</sup>

$$\sigma(E_x) \sim \sum_f |\langle \phi_i | X | \phi_f \rangle|^2 \delta(E_i + E_x - E_f), \quad (1)$$

where  $E_x$ ,  $E_i$ , and  $E_f$  are, respectively, the energy of the photon, the initial state, and the final state.  $X$  is the perturbation acting on the system, which in this case is the absorption process of the photon, for which we will use the dipole approximation.<sup>3</sup>  $\phi_i$  and  $\phi_f$  are the initial- and final-state wave functions. In the single-particle DOS approach,  $\phi_i$  is taken as a core state and  $\phi_f$  is an empty state, which is coupled via the dipole selection rules. For 2p x-ray absorption, the dipole-allowed transitions are  $2p \rightarrow 3d$  and  $2p \rightarrow 4s$ , but as transitions to 3d states dominate over transitions to 4s states, the latter will be neglected. This leads to the expression

$$\sigma_{2p}(E_x) \sim |\langle \phi(2p) | X | \phi(3d) \rangle|^2 \mathcal{P}_{3d}(E_x - E_{2p}), \quad (2)$$

where  $\mathcal{P}_{3d}(E)$  is the unoccupied 3d-projected DOS. The (projected) DOS is normally calculated using density-functional theory (DFT).<sup>4</sup> For the description of x-ray absorption, real-space multiple-scattering (MS) methods,

which have been shown to be equivalent to DFT,<sup>5</sup> are also used.

We follow another approach in treating the x-ray-absorption cross section. Our main assumption is that for 3d transition-metal compounds, the 3d-3d as well as the 2p-3d two-particle interactions are most important for the description of the 2p XAS spectrum. It is these two-particle interactions which define the ground state of the transition-metal ion and which split the XAS final state into a large number of configurations. In the single-particle DOS approximations, the 3d-3d and 2p-3d two-particle interactions are not included. Because we want to calculate them explicitly, we start with the calculation of the atomic multiplets, thereby neglecting all solid-state effects. In the atomic approach the 2p XAS cross section for  $3d^N$  transition-metal ions is,

$$\sigma_{2p}(E_x) \sim \sum_j |\langle \phi_G(3d^N)_{O(3)} | X | \phi_{fj}(2p^5 3d^{N+1})_{O(3)} \rangle|^2 \delta(E_G + E_x - E_f), \quad (3)$$

where  $\phi_G(3d^N)_{O(3)}$  is the ground state of the  $3d^N$  multiplet in spherical [O(3)] symmetry.  $\phi_{fj}(2p^5 3d^{N+1})_{O(3)}$  is state  $j$  in the final-state atomic multiplet spectrum. To include solid-state effects, a cubic-crystal-field term is added to the Hamiltonian. The cubic-crystal-field coupling is treated as a free parameter to be varied to obtain the best fit to experiment. Distortions from cubic symmetry are not considered.

In Sec. II we repeat some general aspects of atomic multiplet theory as far as what is important for partly filled initial states. In Sec. III we will present an overview of the effect of the cubic crystal field on the  $3d^N$  to  $2p^5 3d^{N+1}$  excitation for 14 common valencies of transition-metal ions. We will use crystal-field strengths between 0 and 2.5 eV. As examples for the validity of our method, we will compare the results with some high-

resolution experimental results of  $3d$  transition-metal fluorides in Sec. IV. Section V describes possible reasons for discrepancies and possible refinements.

## II. THEORY

The calculations consist of three steps. First, the energy levels in the initial-state  $3d^N$  multiplet and the final-state  $2p^5 3d^{N+1}$  multiplet are calculated in  $O(3)$  symmetry. Then the atomic multiplet spectrum is calculated by means of the dipole transition from the ground state (in the initial-state multiplet) to all final states. The third part is the projection of the  $O(3)$  multiplets to cubic ( $O_h$ ) symmetry.

### A. Atomic multiplet spectrum

The Hamiltonian of the  $3d^N$  initial-state multiplet consists only of the  $3d$ - $3d$  Coulomb interaction ( $H_{dd}$ ), which is developed in spherical harmonics.<sup>6</sup> The radial parts  $F_{dd}^0$ ,  $F_{dd}^2$ , and  $F_{dd}^4$  are calculated within the Hartree-Fock (HF) limit and corrected by hand to 80% of the HF result to include intra-atomic configuration interaction (CI).<sup>7</sup> The isotope interaction ( $f_0 F^0$ ) does not affect the multiplet, but causes a shift in the average energy position. Our calculation is not suited for the calculation of the absolute energy position. Therefore, we simply shift our calculated multiplet for comparison to experiment. The multiplet splitting is determined by the multipole terms of the  $3d$ - $3d$  interaction,  $F_{dd}^2$  and  $F_{dd}^4$ , which also determine the Hund's-rule ground state within the initial-state  $3d^N$  multiplet.<sup>8</sup> The  $3d$  spin-orbit coupling is small and is neglected as hybridization and temperature effects will mix the spin-orbit-split states.

The  $2p^5 3d^{N+1}$  final-state Hamiltonian is extended with two terms related to the  $2p$  core hole: first, the spin-orbit coupling of the  $2p$  hole ( $H_{cLS}$ ), which causes the division of the  $2p$  edge into the  $2p_{3/2}$  ( $L_3$ ) and  $2p_{1/2}$  ( $L_2$ ). In our calculation we will always consider the full  $2p$ , thus  $L_{2,3}$ , spectrum. The second term which originates from the core hole is the  $2p$ - $3d$  Coulomb and exchange interaction ( $H_{cd}$ ). Again, the radial parts of the  $2p$ - $3d$  Coulomb ( $F_{pd}^0$  and  $F_{pd}^2$ ) and exchange ( $G_{pd}^1$  and  $G_{pd}^3$ ) multipole interactions are calculated *ab initio*. The isotropical  $2p$ - $3d$  Coulomb interaction  $f_0 F_{pd}^0$  is equal for all final states (in a specific  $2p^5 3d^{N+1}$  multiplet). The total Hamiltonian for the atomic multiplet then is

$$H_A = H_{dd} + H_{cLS} + H_{cd}.$$

### B. Cubic-crystal-field effect on the $2p^5 3d^{N+1}$ multiplet

To simulate the solid we add an extra term to the Hamiltonian describing the cubic crystal field ( $H_{CCF}$ ). In the present calculations we assume that the cubic-crystal-field parameter ( $10Dq$ ) is equal for initial and final states.

In terms of group theory, the effect of a cubic crystal field is the reduction of symmetry from  $O(3)$  to  $O_h$ . The group-theoretical treatment of the transformation from  $O(3)$  symmetry to its subgroup  $O_h$ , further called  $O(3)$ - $O_h$

branching, can be found in Refs. 9–11. In our paper on the  $d^0$  compounds, we considered it in more detail.<sup>12</sup>

The cubic crystal field splits the initial-state multiplet. For small cubic crystal fields, the ground state does not change character and originates from the atomic ground state, which according to Hund's rules is high spin. For strong crystal fields a change of character can occur and the ground state can become low spin. That is, it originates from an excited state in the initial-state atomic multiplet. The general results of the influence of the cubic crystal field on the initial-state  $3d^N$  multiplet can be found in the Tanabe-Sugano diagrams.<sup>13</sup>

The crystal field also splits the final-state multiplet. If the character of the ground state is not changed from the atomic situation, the same final states are reached. In this case the changes in the spectrum are a result from the crystal-field effect on the final state. Levels are split and/or shifted, and the transition matrix elements are modified due to changes in the final-state wave functions. This modifies the spectrum. If a change of the ground-state character occurs, this is immediately visible in the spectral shape as the dipole transitions from this new ground state reach a totally new set of final states. The dipole transition operator is not split in cubic symmetry, which means that no polarization dependence can occur.

In the Hamiltonian we neglect all other crystal-field couplings related to lower symmetries, taken together in  $H_{LCF}$ , the  $3d$  spin-orbit coupling, ( $H_{LS}$ ), magnetic interactions ( $H_{ex}$ ), and any form of CI, intra-atomic (e.g.,  $3d^{N-1}4p$ ) as well as extra-atomic (e.g.,  $3d^{N+1}L$ ).  $H_{LCF}$ ,  $H_{LS}$ , and  $H_{ex}$  all will influence the ground-state character. But for the total, polarization-averaged XAS spectrum their influence is negligible as the effects on the final-state multiplet are too small. However, for polarization-dependent XAS measurements, a more accurate determination of the character of the ground state is needed and some extra terms will have to be added to the Hamiltonian. In Sec. V we will discuss possible refinements of the calculations in more detail.

## III. CALCULATIONS

The intra-atomic interaction parameters, as calculated in the Hartree-Fock limit, are collected in Table I. The Coulomb and exchange parameters ( $F_{dd}^2$ ,  $F_{dd}^4$ ,  $F_{pd}^2$ ,  $G_{pd}^1$ , and  $G_{pd}^3$ ) are renormalized to 80% of the HF values to account for intra-atomic CI. The multiplet of the  $3d^N$  initial state and the  $2p^5 3d^{N+1}$  are calculated, and the ground state  $\phi_G(3d^N)_{O(3)}$  is determined. The XAS cross section is calculated. According to Eq. (3), the result is a series of lines at energies ( $E_G - E_{fj}$ ) with respective intensities  $|\langle \phi_G(3d^N)_{O(3)} | X | \phi_{fj}(2p^5 3d^{N+1})_{O(3)} \rangle|^2$ . Figure 1 gives the atomic multiplet for  $d^5 \text{Mn}^{2+}$ . Addition of the cubic-crystal-field changes the energy positions and matrix elements. Figure 2 shows the result if the cubic-crystal-field parameter ( $10Dq$ ) is 0.9 eV.

To compare with experiment, the spectra have to be broadened. Besides the experimental broadening, there are several intrinsic broadening mechanisms. These include lifetime effects, vibrations, and hybridization (covalency), all of which are compound and final state

dependent. Because of the hundreds of (unresolvable) final states, this creates an enormous problem to solve quantitatively. For compounds with a  $3d^0$  ground state, information of the final-state dependence of the broadening can be found experimentally as each of the main multiplet lines can be resolved.<sup>12</sup> Analysis showed that for fluorides, vibrational broadening dominates, but for ox-

ides, also covalence causes broadening. A general result is that the lifetime broadening of the  $L_2$  part is increased due to the opening of Coster-Kronig Auger decay channels. As a detailed analysis of the broadening is not possible from XAS alone, we decided to use an equal broadening for every line. For the  $L_3$  part, a Lorentzian broadening with  $\sigma=0.1$  eV (Ref. 14) is used; for the  $L_2$

TABLE I. Hartree-Fock values of the parameters used in the multiplet calculation. Given are the multipole terms of the  $3d$ - $3d$  interaction ( $F_{dd}^2$  and  $F_{dd}^4$ ) of the ground and final states. The final-state- $3d$ -spin-orbit interaction ( $L \cdot S_d$ ),  $2p$ -hole-spin-orbit interaction ( $L \cdot S_p$ ), and multipole terms of the  $2p$ - $3d$  interaction ( $F_{pd}^2$ ,  $G_{pd}^1$ , and  $G_{pd}^3$ ). In the actual multiplet calculation, the multipole terms are normalized to 80% of their *ab initio* value, to account for intra-atomic configuration interaction (all values in eV).

| $d_N$ | Ion              | $F_{dd}^2$   |          | $F_{dd}^4$   |         | $L \cdot S_d$ | $L \cdot S_p$ |
|-------|------------------|--------------|----------|--------------|---------|---------------|---------------|
|       |                  | final states | (g.s.)   | final states | (g.s.)  |               |               |
| $d^1$ | Ti <sup>3+</sup> | 10.343       | (0.000)  | 6.499        | (0.000) | 0.027         | 3.776         |
|       | V <sup>4+</sup>  | 11.965       | (0.000)  | 7.554        | (0.000) | 0.042         | 4.650         |
| $d^2$ | V <sup>3+</sup>  | 10.974       | (10.127) | 6.888        | (6.354) | 0.036         | 4.649         |
| $d^3$ | Cr <sup>3+</sup> | 11.596       | (10.777) | 7.270        | (6.755) | 0.047         | 5.667         |
|       | Mn <sup>4+</sup> | 13.177       | (12.416) | 8.299        | (7.820) | 0.066         | 6.845         |
| $d^4$ | Cr <sup>2+</sup> | 10.522       | (9.649)  | 6.552        | (6.002) | 0.041         | 5.668         |
|       | Mn <sup>3+</sup> | 12.210       | (11.415) | 7.649        | (7.148) | 0.059         | 6.845         |
| $d^5$ | Mn <sup>2+</sup> | 11.155       | (10.316) | 6.943        | (6.414) | 0.053         | 6.846         |
|       | Fe <sup>3+</sup> | 12.818       | (12.043) | 8.023        | (7.535) | 0.074         | 8.199         |
| $d^6$ | Fe <sup>2+</sup> | 11.779       | (10.966) | 7.327        | (6.815) | 0.067         | 8.200         |
|       | Co <sup>3+</sup> | 13.422       | (12.663) | 8.395        | (7.917) | 0.092         | 9.748         |
| $d^7$ | Co <sup>2+</sup> | 12.396       | (11.605) | 7.708        | (7.209) | 0.083         | 9.746         |
|       | Ni <sup>3+</sup> | 14.022       | (13.277) | 8.764        | (8.295) | 0.112         | 11.506        |
| $d^8$ | Ni <sup>2+</sup> | 0.000        | (12.234) | 0.000        | (7.598) | 0.102         | 11.507        |
| $d^N$ | Ion              | $F_{pd}^2$   |          | $G_{pd}^1$   |         | $G_{pd}^3$    |               |
| $d^1$ | Ti <sup>3+</sup> | 5.581        |          | 3.991        |         | 2.268         |               |
|       | V <sup>4+</sup>  | 6.759        |          | 5.014        |         | 2.853         |               |
| $d^2$ | V <sup>3+</sup>  | 6.057        |          | 4.392        |         | 2.496         |               |
| $d^3$ | Cr <sup>3+</sup> | 6.526        |          | 4.788        |         | 2.722         |               |
|       | Mn <sup>4+</sup> | 7.658        |          | 5.776        |         | 3.288         |               |
| $d^4$ | Cr <sup>2+</sup> | 5.841        |          | 4.024        |         | 2.388         |               |
|       | Mn <sup>3+</sup> | 6.988        |          | 5.179        |         | 2.945         |               |
| $d^5$ | Mn <sup>2+</sup> | 6.321        |          | 4.606        |         | 2.618         |               |
|       | Fe <sup>3+</sup> | 7.446        |          | 5.566        |         | 3.166         |               |
| $d^6$ | Fe <sup>2+</sup> | 6.793        |          | 5.004        |         | 2.844         |               |
|       | Co <sup>3+</sup> | 7.900        |          | 5.951        |         | 3.386         |               |
| $d^7$ | Co <sup>2+</sup> | 7.260        |          | 5.397        |         | 3.069         |               |
|       | Ni <sup>3+</sup> | 8.350        |          | 6.332        |         | 3.603         |               |
| $d^8$ | Ni <sup>2+</sup> | 7.721        |          | 5.787        |         | 3.291         |               |

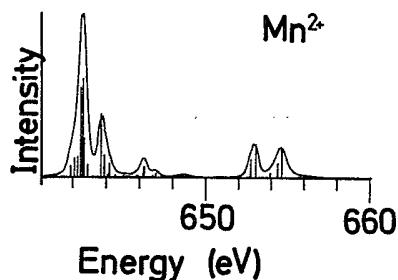


FIG. 1.  $\text{Mn}^{2+} 3d^5$  to  $2p^5 3d^6$  atomic multiplet spectrum. The line spectrum is broadened as described in the text.

part,  $\sigma = 0.3$  eV. Then the spectra are convoluted with a Gaussian with  $\sigma = 0.15$  eV. We expect these broadening procedures to represent early transition-metal fluoride spectra taken with the present high-resolution monochromators.<sup>1</sup> Oxide and late transition-metal fluoride spectra will in general be broader (see Sec. V). Figures 1 and 2 show the effect of the broadening procedure on the two  $\text{Mn}^{2+}$  multiplet spectra.

Figures 3–16 show the effect of increasing cubic crystal field on the x-ray-absorption spectrum. The calculated energy scale is used; for comparison to experiment the spectra will have to be shifted over some eV (see Sec. IV). The  $10Dq$  value is given on the right. The changes as a function of  $10Dq$  are in general smooth and reflect the influence of the cubic crystal field on the final-state multiplet as discussed in Sec. II. In cases where the ground state changes character, from high to low spin, a sudden change in the spectral shape occurs as a new subset of final states is reached. This is visible for, e.g.,  $\text{Cr}^{2+} (d^4)$  and  $\text{Co}^{3+} (d^6)$  between 2.1 and 2.4 eV. Because of the clear difference between high- and low-spin spectra, the actual situation is easy to determine from experiment. Some care has to be taken because the presented calculations are performed in a standard way and do not give the  $10Dq$  value for this transition very accurately. Furthermore,  $10Dq$  can be slightly different in initial and final states. There is no problem to include this, but it does need dedicated, compound-specific calculations.

Two ions with an equal number of  $3d$  electrons, such as  $d^1 \text{V}^{4+}$  and  $\text{Ti}^{3+}$ , have a similar atomic multiplet spectrum. The only differences are the atomic parameter values of the intra-atomic interactions (see Table I),

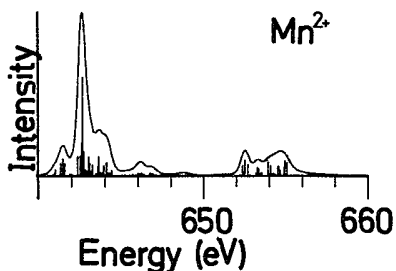


FIG. 2.  $\text{Mn}^{2+} 3d^5$  to  $2p^5 3d^6$  multiplet spectrum, projected to  $O_h$ . The cubic-crystal-field parameter ( $10Dq$ ) is 0.9 eV. The line spectrum is broadened as described in the text.

which slightly modify the spectra.

However, more important is the fact that multiplets do change significantly as the number of  $3d$  electrons is changed. Compare for example,  $\text{Mn}^{2+}$ ,  $\text{Mn}^{3+}$ , and  $\text{Mn}^{4+}$ . Besides the shift to higher energy with higher valency, the spectral shape does change significantly, which makes determination of the valency, and its cubic-crystal-field splitting, straightforward.

#### IV. COMPARISON TO EXPERIMENT

To show the validity of our approach, we make a comparison to some high-resolution  $2p$  x-ray-absorption data of transition-metal fluorides obtained with the Dragon monochromator by Chen and Sette.<sup>15</sup>

In our paper on the  $3d^0$  compounds, we showed the excellent agreement with potassium, calcium, scandium, and titanium oxides and fluorides. As the final-state  $p^5 d^1$  is simple and well resolved, it was possible to obtain detailed information, such as individual broadenings for each state. Such detailed analysis is not possible for the  $p^5 d^{N+1}$  multiplets (for  $N > 0$ ), as the individual lines are not resolved (there are typically 600 lines spread over 20 eV). Therefore, the standard broadening as discussed in Sec. III is used.

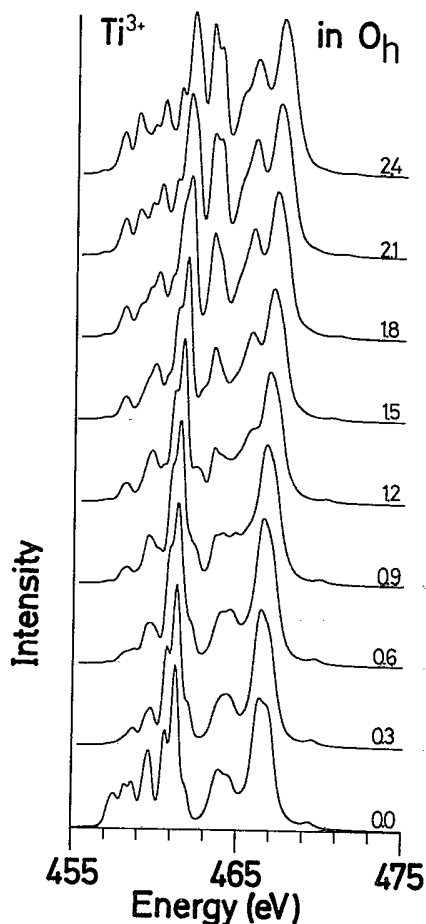


FIG. 3.  $\text{Ti}^{3+} 3d^1$  to  $2p^5 3d^2$  transition in cubic crystal fields.  $10Dq$  ranges from 0.0 (bottom) to 2.4 eV.

In Fig. 17 the theoretical spectra of  $V^{3+}$  ( $d^2$ ),  $Mn^{2+}$  ( $d^5$ ), and  $Co^{2+}$  ( $d^7$ ) are compared with the experimental spectra of  $VF_3$ ,  $MnF_2$ , and  $CoF_2$  (see Table II for the crystal structures) as obtained with the Dragon,<sup>15</sup> The cubic-crystal-field parameters ( $10Dq$ ) used are, respectively, 1.5, 0.75, and 0.75 eV. The overall agreement found is good for all compounds. From this we conclude that the atomic multiplet approach with the inclusion of the cubic crystal field gives a good description of all spectral details of the 2p x-ray-absorption spectra of 3d transition-metal fluorides. This also shows that the tetragonal symmetry of the metal site in  $CoF_2$  and  $MnF_2$  (Table II) is a too-small distortion from cubic symmetry to cause clear disagreement between experiment and the present cubic symmetry simulation. However, for the description of polarization-dependent spectra of a tetragonal site, the inclusion of the exact lower symmetry is absolutely necessary. In other words, with polarization-dependent measurements small tetragonal distortions will show up. Unfortunately, a rutile crystal structure is not suitable for polarization-dependent studies because of different orientations of the tetragonal sites.

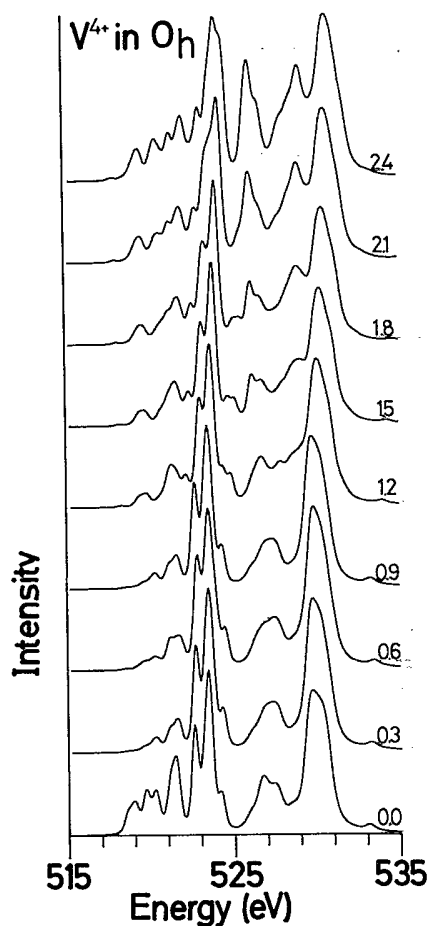


FIG. 4.  $V^{4+}$   $3d^1$  to  $2p^5 3d^2$  transition in cubic crystal fields.  $10Dq$  ranges from 0.0 (bottom) to 2.4 eV.

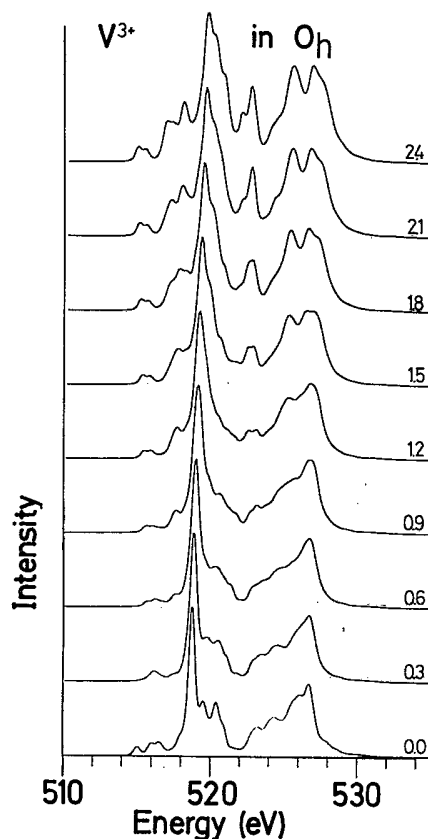


FIG. 5.  $V^{3+}$   $3d^2$  to  $2p^5 3d^3$  transition in cubic crystal fields.  $10Dq$  ranges from 0.0 (bottom) to 2.4 eV.

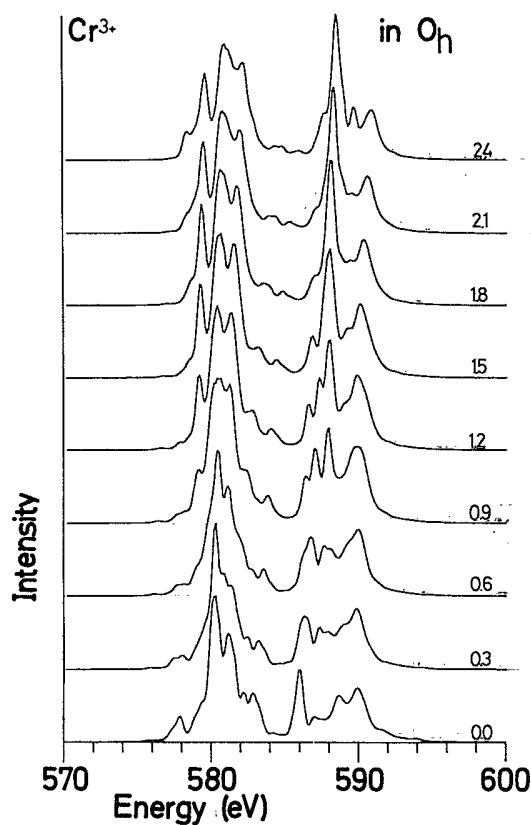


FIG. 6.  $Cr^{3+}$   $3d^3$  to  $2p^5 3d^4$  transition in cubic crystal fields.  $10Dq$  ranges from 0.0 (bottom) to 2.4 eV.

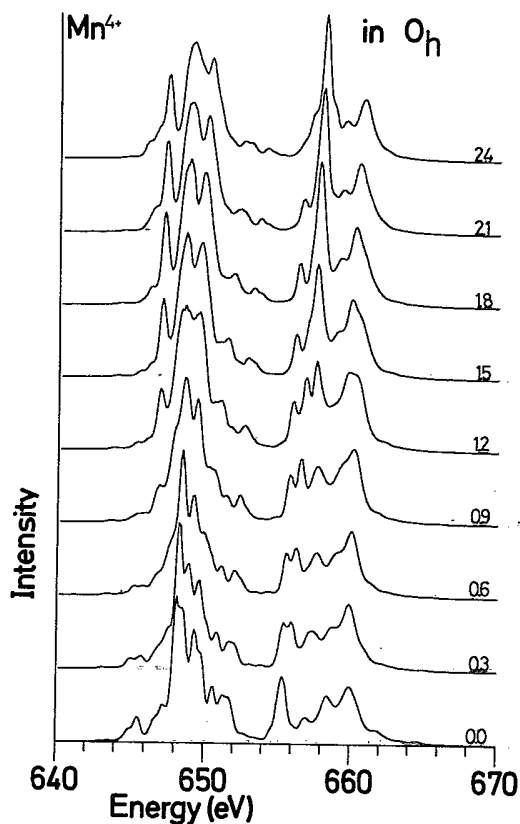


FIG. 7.  $\text{Mn}^{4+} 3d^3$  to  $2p^5 3d^4$  transition in cubic crystal fields.  $10Dq$  ranges from 0.0 (bottom) to 2.4 eV.

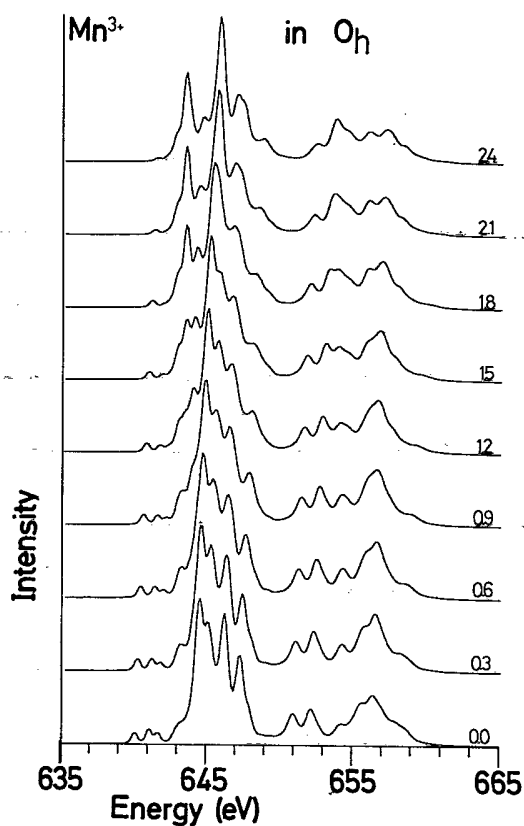


FIG. 9.  $\text{Mn}^{3+} 3d^4$  to  $2p^5 3d^5$  transition in cubic crystal fields.  $10Dq$  ranges from 0.0 (bottom) to 2.4 eV.

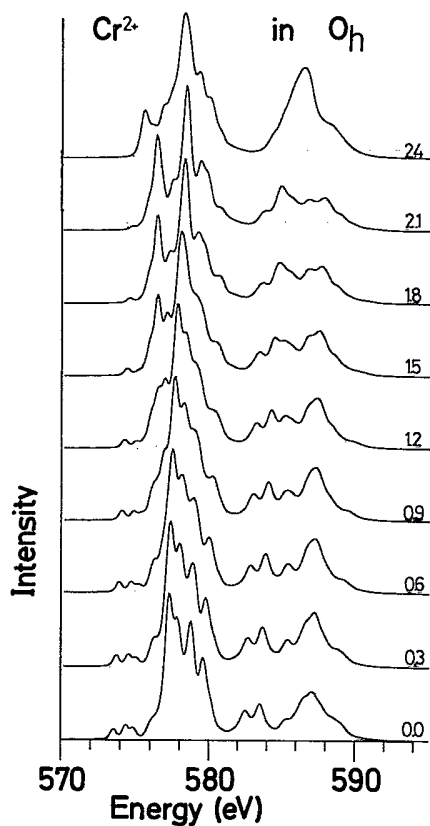


FIG. 8.  $\text{Cr}^{2+} 3d^4$  to  $2p^5 3d^5$  transition in cubic crystal fields.  $10Dq$  ranges from 0.0 (bottom) to 2.4 eV.

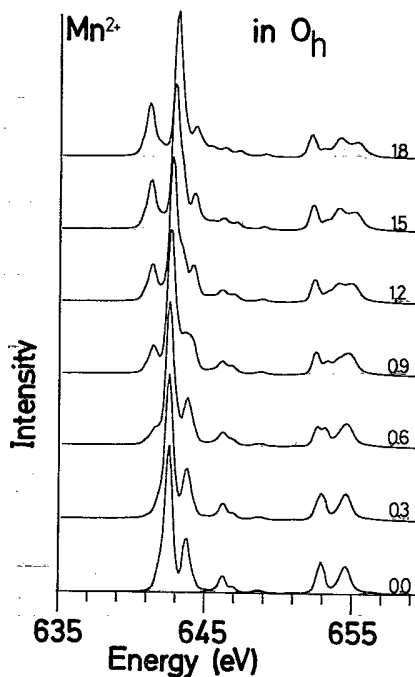


FIG. 10.  $\text{Mn}^{2+} 3d^5$  to  $2p^5 3d^6$  transition in cubic crystal fields.  $10Dq$  ranges from 0.0 (bottom) to 1.8 eV.

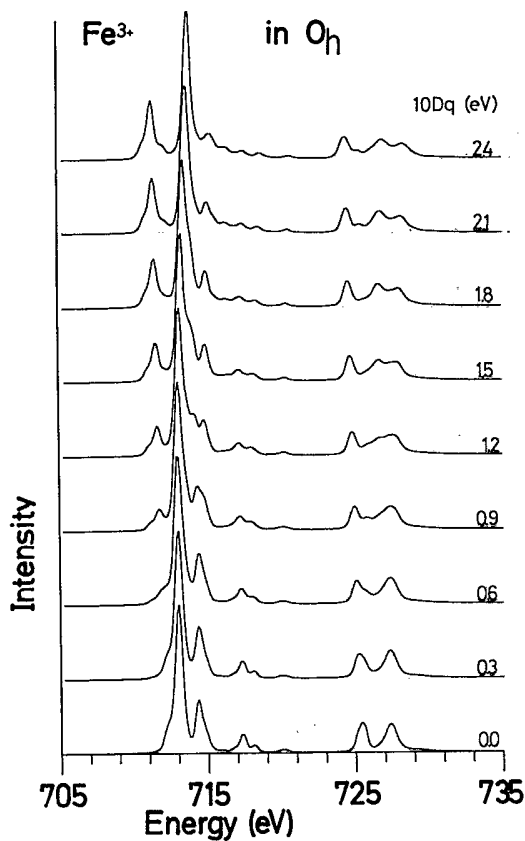


FIG. 11.  $\text{Fe}^{3+} 3d^5$  to  $2p^5 3d^6$  transition in cubic crystal fields.  $10Dq$  ranges from 0.0 (bottom) to 2.4 eV.

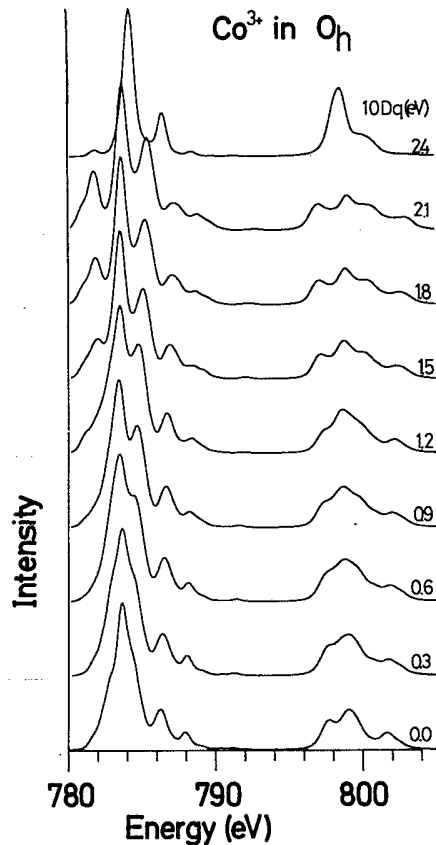


FIG. 13.  $\text{Co}^{3+} 3d^6$  to  $2p^5 3d^7$  transition in cubic crystal fields.  $10Dq$  ranges from 0.0 (bottom) to 2.4 eV.

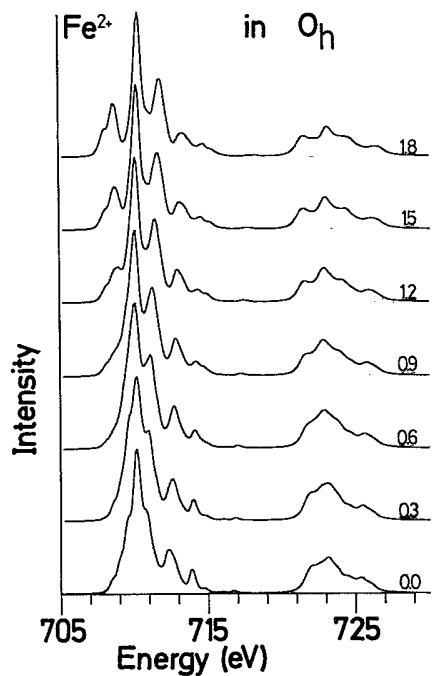


FIG. 12.  $\text{Fe}^{2+} 3d^6$  to  $2p^5 3d^7$  transition in cubic crystal fields.  $10Dq$  ranges from 0.0 (bottom) to 1.8 eV.

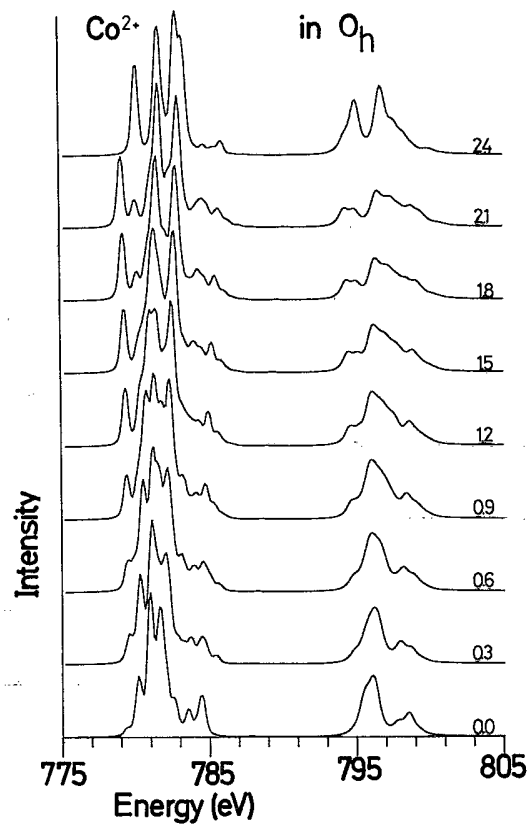


FIG. 14.  $\text{Co}^{2+} 3d^7$  to  $2p^5 3d^8$  transition in cubic crystal fields.  $10Dq$  ranges from 0.0 (bottom) to 2.4 eV.

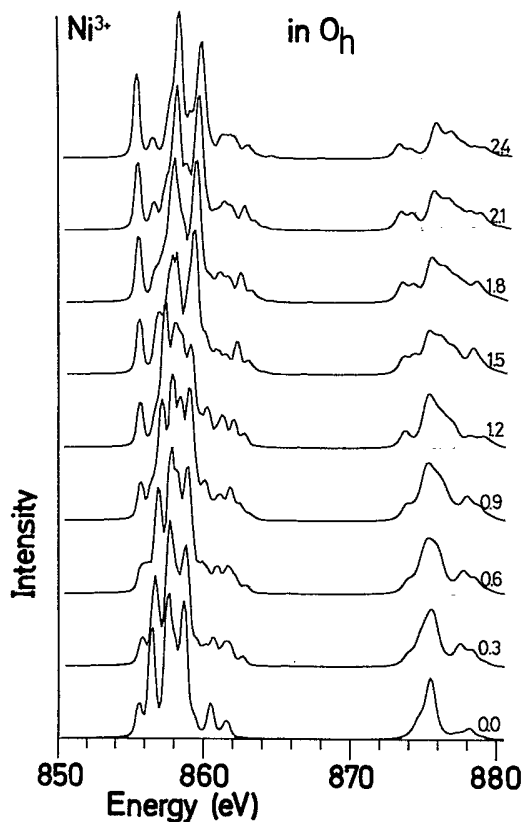


FIG. 15.  $\text{Ni}^{3+} 3d^7$  to  $2p^5 3d^8$  transition in cubic crystal fields.  $10Dq$  ranges from 0.0 (bottom) to 2.4 eV.

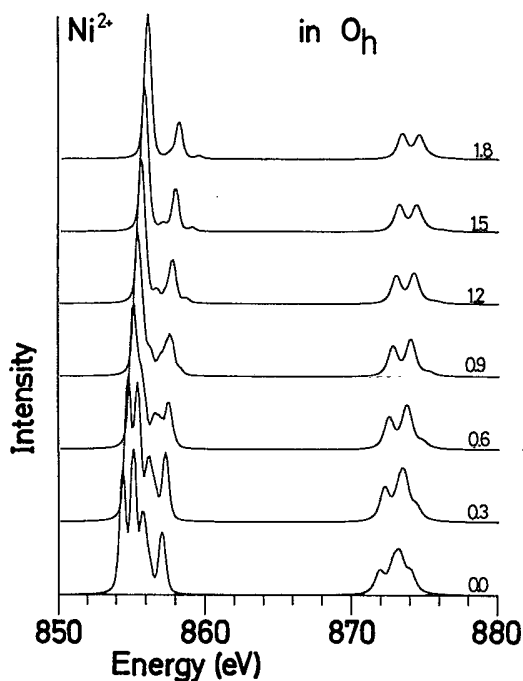


FIG. 16.  $\text{Ni}^{2+} 3d^8$  to  $2p^5 3d^9$  transition in cubic crystal fields.  $10Dq$  ranges from 0.0 (bottom) to 2.4 eV.

## V. LIMITATIONS OF THIS APPROACH

There are two main limitations in the present approach to explain the  $2p$  x-ray-absorption edges. First, the character of the ground state is not considered in detail. Second, the effects on the spectral shape of hybridization, vibrations, lifetime, and experimental resolution are treated very roughly as a general Lorentzian-plus-Gaussian broadening.

In Sec. II we already mentioned the necessity to include the exact lower-site symmetries ( $H_{LCF}$ ), magnetic

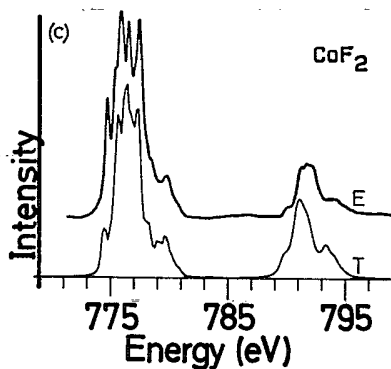
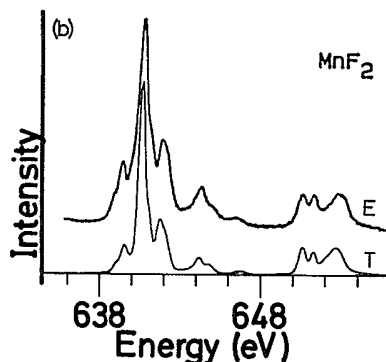
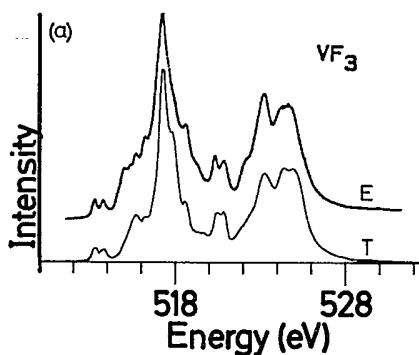


FIG. 17.  $2p$  x-ray-absorption spectra of (a)  $\text{VF}_3$ , (b)  $\text{MnF}_2$ , and (c)  $\text{CoF}_2$  compared, respectively, with the  $d^2\text{V}^{3+}$  (1.5 eV), the  $d^5\text{Mn}^{2+}$  (0.75 eV), and the  $d^7\text{Co}^{2+}$  (0.75 eV) multiplet calculations. The used values of  $10Dq$  are given in parentheses. The theoretical spectra are shifted, by about 2 eV to lower energy, to align with experiment.



TABLE II. Crystal structures of the 3d transition-metal fluorides (Ref. 26).

| Compound         | Crystal structure           | Point group of metal ion     |
|------------------|-----------------------------|------------------------------|
| VF <sub>3</sub>  | (intermediate) close packed | O <sub>h</sub> (octahedral)  |
| MnF <sub>2</sub> | rutile                      | D <sub>4h</sub> (tetragonal) |
| CoF <sub>2</sub> | rutile                      | D <sub>4h</sub> (tetragonal) |

field effects ( $H_{ex}$ ), and 3d spin-orbit coupling ( $H_{LS}$ ) to describe the character of the ground state more accurately.  $H_{LCF}$  and  $H_{ex}$  will not influence the polarization-averaged spectral shape because the effects are generally too small to be seen in the final-state multiplet. That is, even if they modify the ground-state character considerably, the polarization-averaged (!) matrix elements hardly change. Only for strongly distorted sites can a visible effect be expected. However, for the polarization-dependent spectra, knowledge of the ground-state character is crucial for the determination of the respective matrix elements for  $\Delta m = +1$ ,  $-1$ , or  $0$ .<sup>16,17</sup> Then the interplay of  $H_{LCF}$ ,  $H_{ex}$ , and  $H_{LS}$  will determine the exact ground state and, consequently, the differences in spectral shape for linear (difference between  $\Delta m = 0$  and  $+1/-1$ ) and circular (difference between  $\Delta m = 1$  and  $-1$ ) dichroism.

The 3d spin-orbit coupling might influence the spectral shape for solids. Its influence on the polarization-averaged spectra will be directly evident from the branching ratio between  $L_3$  and  $L_2$ .<sup>18</sup> Its influence will be largest, if present at all, for the late 3d transition metals (see Table I), and indeed for CoF<sub>2</sub> [see Fig. 17(c)] the branching ratio, as well as the total spectral shape, is improved if the 3d spin-orbit coupling is included.<sup>19</sup>

We now turn to the second limitation, the use of an equal broadening for all final states in the  $L_3$  and  $L_2$  parts to simulate effects such as hybridization, vibrations, and lifetime. These effects will be different for every compound and even for every line in the 600-line final-state multiplet, making a detailed description totally out of reach. However, some aspects are becoming clear: For the  $d^0$  compounds it was shown that the  $e_g$ -like states show more broadening than the  $t_{2g}$ -like states, which we related to vibrational effects. For the  $2p^5 3d^{N+1}$  multiplets such conclusions cannot be drawn, but similar effects can be expected.

Hybridization, which can be treated as extra-atomic configuration interaction, will modify the spectrum considerably. Especially for more covalent materials, such as oxides, the amount of extra-atomic configuration interaction cannot be neglected: The coupling of  $3d^N$  with  $3d^{N+1}\bar{L}$  becomes more prominent, introducing more  $3d^{N+1}\bar{L}$  character in the ground state. These aspects can be taken into account by performing a real CI calculation, as was done for the early 3d transition metals<sup>20</sup> and for the nickel-dihalides.<sup>21</sup> For the cases considered here, such a CI approach is at present not a routine task, but this line will certainly be followed in future efforts.

An alternative route is to include the effects of hybridization effectively in the atomic multiplet calculations. Hybridization, the mixing of the transition-metal 3d orbitals with the ligand  $p$  orbitals, has the effect of delocal-

izing the  $d$  functions, thereby reducing their mutual interactions: the nephelauxatic effect.<sup>22</sup> This effect can be simulated by an extra reduction of the two-particle interaction parameters  $F_{dd}^2$  and  $F_{dd}^4$ . Also the final-state interactions with the core hole will be affected. Preliminary calculations, where we reduced all parameters by the same amount, are encouraging, although the possible accuracy has to be investigated,<sup>23</sup> and shake-up satellites will not be reproduced properly.

The last effect which is not treated in detail is the lifetime broadening. It can be expected that the lifetime is different for about everyone of the 600 final states. The states at higher energy can lose energy by Coster-Kronig-like Auger decay to lower states, and the other decay routes will be different also. This problem relates to the more general question of the coupling of core-hole creation and decay, and its influence on the spectral shape of the different spectroscopic techniques. The answer will have to be formed by a combination of normal x-ray absorption and x-ray photoemission with "resonance" experiments, in which the x-ray energy is scanned through the  $L_{2,3}$  XAS energy range, and the resulting x-ray-emission spectra,<sup>24</sup> Auger spectra,<sup>25</sup> and/or photoemission spectra are measured.

## VI. CONCLUDING REMARKS

We have shown that the atomic multiplet approach with the inclusion of the cubic crystal field reproduces the metal 2p x-ray-absorption spectra of 3d transition-metal fluorides. For more covalent compounds, such as oxides, the presented spectra are probably less accurate, although this remains to be checked. As discussed, this can be improved upon by an effective reduction of the 3d-3d Coulomb interactions. By comparison to experiment an accurate measure of the crystal-field-strength parameter  $10Dq$  can be obtained. In fact, the final-state value of  $10Dq$  is found, which can be different from the "initial"-state values that are found by optical spectroscopy. A study of this would be of quite some interest.

The field of application of the atomic multiplet plus crystal-field approach as presented here will probably be limited to the more ionic 3d transition-metal compounds. For the pure metals and alloys, band-structure effects may be of equal or greater importance than the atomic multiplet effects.<sup>20</sup> A systematic experimental study of band-versus-atomic effects would be of great interest in this regard.

## ACKNOWLEDGMENTS

We are grateful to C. T. Chen and Francesco Sette for making available their unpublished results of the

transition-metal fluorides, taken with the high-resolution Dragon monochromator. This study was supported in part by the Dutch Foundation for Chemical Research [Stichting Scheikundig Onderzoek in Nederland (SON)] with financial assistance of the Netherlands Organization

for Scientific Research [Nederlandse Organisatie voor wetenschappelijk Onderzoek (NWO)], and by the Committee for the European Development of Science and Technology (CODEST) Program.

- <sup>1</sup>A resolution up to 1:10 000 is reached by the Dragon monochromator at Brookhaven National Laboratory (Upton, NY): C. T. Chen, *Nucl. Instrum. Methods A* **256**, 595 (1987). Other high-resolution monochromators in the 300–800-eV range include the SX700 at BESSY, Berlin: H. Petersen, *ibid.* **246**, 260 (1986); and the 10-m-focal-length grazing-incidence monochromator at the Photon Factory: H. Maezawa, S. Nakai, S. Mitani, A. Mikuni, T. Namioka, and T. Sasaki, *ibid.* **246**, 310 (1986).
- <sup>2</sup>T. Yamaguchi, S. Shibuya, and S. Sugano, *J. Phys. C* **15**, 2625 (1982), T. Yamaguchi, S. Shibuya, S. Suga, and S. Shin, *ibid.* **15**, 2641 (1982).
- <sup>3</sup>S. Gasiorowicz, *Quantum Physics* (Wiley, New York, 1974), Chap. 22.
- <sup>4</sup>The use of DFT for x-ray absorption is worked out in J. E. Müller and J. W. Wilkins, *Phys. Rev. B* **29**, 4331 (1984).
- <sup>5</sup>C. R. Natoli and M. Benfatto, *J. Phys. Colloq.* **47**, C8-11 (1986).
- <sup>6</sup>The theoretical basis for this method can be found in R. D. Cowan, *J. Opt. Soc. Am.* **58**, 808 (1968), and R. D. Cowan, *The Theory of Atomic Structure and Spectra* (University of California Press, Berkeley, 1981).
- <sup>7</sup>R. D. Cowan, *The Theory of Atomic Structure and Spectra* (University of California Press, Berkeley, 1981), p. 464, and references therein.
- <sup>8</sup>See, e.g., C. J. Ballhausen, *Introduction to Ligand Field Theory* (McGraw-Hill, New York, 1962).
- <sup>9</sup>P. H. Butler, *Point Group Symmetry, Applications, Methods and Tables* (Plenum, New York, 1981).
- <sup>10</sup>J. R. Derome and W. T. Sharp, *J. Math. Phys.* **6**, 1584 (1965).
- <sup>11</sup>P. H. Butler and B. G. Wybourne, *Int. J. Quantum Chem.* **10**, 581 (1976).
- <sup>12</sup>F. M. F. de Groot, J. C. Fuggle, B. T. Thole, and G. A. Sawatzky, *Phys. Rev. B* **41**, 928 (1990).
- <sup>13</sup>S. Sugano, Y. Tanabe, and H. Kamimura, *Multiplets of Transition Metal Ions in Crystals* (Academic, New York, 1970), Chap. 5.1.
- <sup>14</sup>For the late 3d transition metals, the Lorentzian broadening of 0.1 eV is too small, as only lifetime effects will cause a larger broadening. See, e.g., J. C. Fuggle and S. Alvarado, *Phys. Rev. A* **22**, 1615 (1980), and references therein.
- <sup>15</sup>C. T. Chen and F. Sette (private communication).
- <sup>16</sup>R. D. Cowan, Ref. 7, p. 403.
- <sup>17</sup>We have made several observations of such effects in cooperation with various other groups, and these will be published in the near future.
- <sup>18</sup>B. T. Thole and G. van der Laan, *Phys. Rev. B* **38**, 3158 (1988).
- <sup>19</sup>F. M. F. de Groot (unpublished).
- <sup>20</sup>J. Fink, Th. Müller-Heinzerling, B. Scheerer, W. Speier, F. U. Hillebrecht, J. C. Fuggle, J. Zaanen, and G. A. Sawatzky, *Phys. Rev. B* **32**, 4899 (1985); J. Zaanen, G. A. Sawatzky, J. Fink, W. Speier, and J. C. Fuggle, *ibid.* **32**, 4905 (1985).
- <sup>21</sup>J. Zaanen, C. Westra, and G. A. Sawatzky, *Phys. Rev. B* **33**, 8060 (1986).
- <sup>22</sup>C. K. Jorgensen, *Absorption Spectra and Chemical Bonding in Complexes* (Pergamon, Oxford, 1962), Chap. 8.
- <sup>23</sup>F. M. F. de Groot *et al.* (unpublished).
- <sup>24</sup>J.-E. Rubensson, D. Mueller, R. Schuker, D. L. Ederer, C. H. Zhang, J. Jia, and T. A. Callcott, *Phys. Rev. Lett.* **64**, 1047 (1990).
- <sup>25</sup>D. D. Sarma, C. Carbone, P. Sen, and W. Gudat, *Phys. Rev. B* **40**, 12 542 (1989).
- <sup>26</sup>A. F. Wells, *Structural Inorganic Chemistry*, 4th ed. (Clarendon, Oxford, 1975), pp. 350–355, and references therein.